Notch and Hedgehog in the thymus/parathyroid common primordium

Figueiredo, Marta; Silva, Joana Clara; Santos, Ana Sofia; Proa, Vitor; Alcobia, Isabel; Zilhão, Rita

Published in:
Developmental Biology

DOI:
10.1016/j.ydbio.2016.08.012

Publication date:
2016

www.elsevier.com/locate/developmentalbiology

Notch and Hedgehog in the thymus/parathyroid common primordium: Crosstalk in organ formation

Marta Figueiredo, Joana Clara Silva, Ana Sofia Santos, Vitor Proa, Isabel Alcobia, Rita Zilhão, António Cidadão, Hélia Neves

PII: S0012-1606(15)30229-3
DOI: http://dx.doi.org/10.1016/j.ydbio.2016.08.012
Reference: YDBIO7224

To appear in: *Developmental Biology*

Received date: 6 October 2015
Revised date: 12 August 2016
Accepted date: 13 August 2016

Cite this article as: Marta Figueiredo, Joana Clara Silva, Ana Sofia Santos, Vitor Proa, Isabel Alcobia, Rita Zilhão, António Cidadão and Hélia Neves, Notch and Hedgehog in the thymus/parathyroid common primordium: Crosstalk in organ formation, *Developmental Biology* http://dx.doi.org/10.1016/j.ydbio.2016.08.012

Notch and Hedgehog in the thymus/parathyroid common primordium: crosstalk in organ formation

Marta Figueiredo[a,b1], Joana Clara Silva[a1,2], Ana Sofia Santos[a,3], Vitor Proa[a], Isabel Alcobia[a,b], Rita Zilhão[c], António Cidadão[a], Hélia Neves[a,b*]

[a]Instituto de Histologia e Biologia do Desenvolvimento, Faculdade de Medicina da Universidade de Lisboa, Edifício Egas Moniz, Piso 3, Ala C, Av. Prof. Egas Moniz, 1649-028 Lisboa, Portugal

[b]Instituto de Medicina Molecular, Faculdade de Medicina da Universidade de Lisboa, Av. Prof. Egas Moniz, 1649-028 Lisboa, Portugal

[c]Departamento de Biologia Vegetal, Faculdade de Ciências da Universidade de Lisboa. Campo Grande C2, 1749-016 Lisboa, Portugal

martafigueiredo@medicina.ulisboa.pt
j.clarasilva@dundee.ac.uk
assantos@hikma.com
vitorproa@medicina.ulisboa.pt
halcobia@medicina.ulisboa.pt
rmzilhao@fc.ul.pt
a.cidadao@campus.ul.pt
helia.neves@campus.ul.pt
hneves@ medicina.ulisboa.pt

[*]Correspondence: Phone +351 21 7999528. Fax +351 21 7999527

Abstract

The avian thymus and parathyroids (T/PT) common primordium derives from the endoderm of the third and fourth pharyngeal pouches (3/4PP). The molecular mechanisms that govern T/PT development are not fully understood. Here we study the effects of Notch and Hedgehog (Hh) signalling modulation during common primordium development using *in vitro*, *in vivo* and *in ovo* approaches. The impairment of Notch activity reduced Foxn1/thymus-fated and Gcm2/Pth/parathyroid-fated domains in the 3/4PP and further compromised the development of the parathyroid glands. When Hh signalling was abolished, we observed a reduction in the *Gata3*/*Gcm2*- and *Lfng*-expression domains at the median/anterior and median/posterior territories of the pouches, respectively. In contrast, the *Foxn1* expression-

[1] Co-authors, these authors contributed equally to this work.
[2] Present Address: JKD Lab, College of Life Sciences, University of Dundee, Dow Street, DD1 5EH, Dundee, UK.
[3] Present Address: Hikma Farmacêutica (Portugal), S.A., Sintra, Portugal.

domain at the dorsal tip of the pouches expanded ventrally into the *Lfng*-expression domain. This study offers novel evidence on the role of Notch signalling in T/PT common primordium development, in an Hh-dependent manner.

Keywords: Notch; Hedgehog; thymus/parathyroids common primordium; pharyngeal pouches; avian.

Introduction

The parathyroid glands and the thymus are organs with distinct functions, carried out mainly by epithelial cells which have a common embryological origin, that is, the endoderm of the pharyngeal pouches (PP). The epithelia of these organs in the avian model originate from the third and fourth PP (3/4PP) endoderm. It is worth noting, that in mammals the thymic epithelium derives from the 3PP endoderm (Farley et al., 2013; Gordon et al., 2001) and in mouse and human the epithelium of parathyroids derives from the 3PP and 3/4PP, respectively. The main function of the parathyroid endocrine epithelium is to secrete a peptidic hormone, the parathyroid hormone (Pth), essential for the regulation of calcium and phosphate homeostasis (Potts, 2005). In the thymus, the epithelial cells establish complex interactions with the developing lymphocytes to produce self-restricted and self-tolerant T-cells, which generate central immune tolerance.

Parathyroid and thymic organogenesis starts with the budding off and outgrowth of rudiments from pouches of the foregut endoderm (Manley and Condie, 2010), accompanied by the lining of neural crest-derived connective tissues (Grevellec and Tucker, 2010). These early steps involve pouch patterning and the establishment of a common primordium (Manley and Condie, 2010) in which the distinct parathyroid and thymic prospective domains, can be distinguished by the expression of the organ-specific genes, Gcm2 (Glial cells missing 2) and Foxn1, respectively.

In avian embryos, *Gcm2* transcripts were first detected by RT-PCR in isolated quail (q) endoderm at embryonic day (E) 2.5 (25-30 somite-stage) (Neves et al., 2012). However, *in situ* expression of *Gcm2* has only been observed in the anterior domain of the 3PP and 4PP at Hamburger and Hamilton Stage 18 (HH18) and HH22, respectively (Okabe and Graham, 2004). This temporal sequence of *Gcm2* expression follows the chronological formation of the pouches. As development proceeds, Pth is upregulated in the developing glands. In avian, *Pth* expression was first observed *in situ* at chicken (c) E5.5 (HH28) (Grevellec et al., 2011). In Gcm2

homozygous null mutant mice, the expression of *Pth* is not initiated and no parathyroid glands are formed (Günther et al., 2000; Liu et al., 2007).

The transcription factor of the winged helix/forkhead class, Foxn1, is the earliest known marker of the thymic rudiment. *Foxn1* transcripts were detected in isolated quail endoderm 24 hours after *Gcm2* expression. At cE4.5, *Foxn1* expression was observed *in situ* in the dorsal tip of the 3/4PP and transcription endures until birth (Neves et al., 2012). The gene is mutated in the nude mouse strain, which displays abnormal hair growth and failure of thymus development, leading to immunodeficiency (Nehls et al., 1996; Blackburn et al., 1996; Bleul et al., 2006).

As in other developmental processes, the activation of the correct transcriptional programs during parathyroid (Neves and Zilhão, 2014) and thymic (Manley and Condie, 2010) organogenesis depends on the crosstalk of several signalling pathways which respond to extracellular signals.

Notch signalling is a major pathway during development that acts in a juxtacrine fashion and is responsible for cell-fate decisions (Lewis, 1998; Lai, 2004). In the last fifteen years, several reports have shown that Notch is fundamental during epithelial-lymphoid cell interactions at late-stages of thymus formation (Rodewald, 2008). Notably, perinatal mutant mice with loss of Notch ligand Jag2 exhibit aberrant thymic morphology with smaller medullar compartments (Jiang et al., 1998). Notch activity is also required for the commitment of lymphoid progenitor cells to the T-cell lineage (Pui et al., 1999; Radtke et al., 1999), in a ligand dependent manner (Jaleco et al., 2001; Dorsch et al., 2002). Whilst largely unknown, there is some evidence for the role of Notch signalling in the early-development of these organs. In mice, the loss of Notch-target Hes1 promotes a spectrum of malformations of pharyngeal endoderm-derived organs, including parathyroid glands aplasia/hypoplasia (Kameda et al., 2013) and abnormal thymic formation (Tomita et al., 1999; van Bueren et al., 2010; Kameda et al., 2013).

Paracrine Hedgehog (Hh) signalling is also involved in craniofacial and neck morphogenesis (Grevellec and Tucker, 2010), and regulates T/PT common primordium development (Moore-Scott and Manley, 2005). In Sonic Hh (Shh) homozygous null mutants the rudiment boundaries are compromised, displaying an expanded domain of the prospective thymic territory at the expense of the Gcm2/parathyroid-fated domain (Moore-Scott and Manley, 2005). This mutant fails to form parathyroid glands (Moore-Scott and Manley, 2005) and displays functional defects in the thymus (Shah et al., 2004). At later stages of development, Shh and Indian Hh, other Hh signalling molecules, are known to regulate thymocyte differentiation after thymic epithelium colonization by lymphoid progenitor cells (Outram et al., 2009).

Hh and Notch pathways interact in multiple biological scenarios (McGlinn et al., 2005; Lawson et al., 2002; Stasiulewicz et al., 2015). In distinct developmental contexts, Notch signalling is known to control morphological boundary formation by the mechanism of lateral inhibition (Lewis, 1998; Lai, 2004; Kiernan, 2013). In light of this evidence, we hypothesized that similar mechanisms could operate in the development of T/PT common primordium. In order to test this hypothesis, Notch and Hh signals were inhibited *in vitro* and *in vivo* in the presumptive territories of thymus and parathyroids by ectopic administration of the respective pharmacological inhibitors. Briefly, our results show a positive regulatory effect of Notch signalling in T/PT common primordium development and parathyroid gland formation. Hh positively regulates the Gata3/Gcm2/parathyroid-fated domain. Furthermore, Hh establishes the dorsal/posterior boundary of Foxn1/thymic rudiment by positively regulating Lfng/Notch signals at the posterior/median territory of the developing 3/4PP endoderm.

Materials and Methods

Embryo preparation

Fertilised Japanese quail (*Coturnix coturnix japonica*) and chicken (*Gallus gallus*) eggs were incubated at 38°C in a humidified incubator. Embryos were staged according to Hamburger and Hamilton (Hamburger and Hamilton, 1951). Quail (q) embryos were dissected at embryonic day (E) 3 and E4 for *in vitro* development studies and whole-mount *in situ* hybridisation (WM-ISH) procedures. Chicken (c) embryos were used at E2.5 (HH17) and E3.5 (HH21) for *in vivo* assays and at E8 for *in ovo* organ formation assays. Chicken pharyngeal endoderm was isolated at E3.5 and E4.5 (HH24-25) and used for WM-ISH, as previously described (Neves et al., 2012).

In vitro organotypic assay

The third and fourth pharyngeal arches region (3/4PAR) was dissected from qE3 on PBS (3/4PAR-0h), and kept on ice until culture. The 3/4PAR included the 3/4PP and foregut endoderm and the ventral mesenchymal- and ectodermal-neighbouring cells. The dorsal structures like notochord, somites and neural tube were removed (Figure 1A-F). Explants were then placed on a 24mm Transwell® with 0.4µm Pore Polycarbonate Membrane Insert (Corning Product #3412). Seven explants per well were placed with the ventral side up and the dorsal side in contact with the membrane (Figure 1G). The tissues were grown partially immersed in culture medium, RPMI-1640 Medium (Sigma) supplemented with 10% FBS (Invitrogen), 1x Pen/Strep (Invitrogen) in a humidified incubator at 37°C with 5% CO_2, for 48h (3/4PAR-48h).

For Notch signalling inhibition assays, culture medium was supplemented with LY-411.575 (Ly, Stemgent - Stemolecule™) at 50nM (Ly-50), 100nM (Ly-100) or 200nM (Ly-200) or with Dibenzazepine (DBZ, Selleckchem) at 5µM (DBZ-5), 10µM (DBZ-10) or 15µM (DBZ-15) (experimental conditions). For Hh signalling inhibition assays, culture medium was supplemented with 20µM of Cyclopamine (Cyc, Sigma) or with 10µM of Vismodegib (Vis, Selleckchem) (experimental conditions). In parallel, explants were grown with culture medium supplemented with the drug solvent, DMSO, at similar concentrations as the ones present in the medium of experimental conditions [Control-50 (Ly)- 0.0005% DMSO; Control-100 (Ly)- 0.001% DMSO; Control-200 (Ly)- 0.002% DMSO; Control-5 (DBZ)- 0.05%; Control-10 (DBZ)- 0.10%; Control-15 (DBZ)- 0.15%; Control (Cyc)- 0.16%; Control (Vis)- 0.2%] (control conditions).

Following the incubation period, cultured explants were either used for RNA isolation (see Quantitative real time RT-PCR section) or grafted on the chorioallantoic membrane (CAM) at cE8.

In ovo organ formation assay

The 3/4PAR explants grown *in vitro* for 48h were grafted on the CAM of chicken embryos at cE8 (Figure 1G). Transplanted tissues were allowed to further develop *in ovo* for 10 days in a humidified incubator at 38°C, as previously described (Neves et al., 2012). For Notch inhibition assays, the 3/4PAR-48h explants derived from Ly-200 (3/4PAR Ly-200) were grafted and developed in CAM (Graft-Ly) (experimental condition). For the control conditions, 3/4PAR-48h explants derived from Control-200 (3/4PAR Control-200) were grafted and developed in CAM (Control-Ly). For both conditions, transplanted tissues were allowed to further develop *in ovo* for 3 and 10 days in a humidified incubator at 38°C. Survival and organ formation were evaluated in CAM-derived explants grown *in ovo* for 10 days.

In vivo assays

For *in vivo* Notch inhibition assays, 20-40µl of 5µM, 10µM or 20µM of Ly were injected on the right side of the embryo near the region of the heart and pharyngeal arches, after local removal of extra-embryonic membranes, at cE2.5 and cE3.5. In parallel, control embryos were injected with 20-40µl of DMSO at a similar concentration as the one present in the medium of experimental conditions (0.05%, 0.1% and 0.2%, respectively). Chicken embryos were allowed to develop *in ovo* for 20-24h in a humidified incubator at 38°C.

For *in vivo* Hh inhibition assays, heparin acrylic beads (Sigma) were rinsed in PBS and soaked overnight at 4°C in a solution of 6mM of Cyc or in PBS. Cyc- and PBS-beads were inserted in the embryo pharynx lumen through the second cleft and placed at the level of the 3/4PP, after local removal of extra-embryonic membranes, at cE2.5 and qE3 (Cyc and Control-PBS, respectively). In order to increase Hh inhibition effects, multiple beads were placed per embryo. Quail embryos were allowed to develop for 20-24h in 30 mm petri-dishes containing 2mL of PBS in a humidified incubator with 5% CO_2 at 37°. Chicken embryos were allowed to develop *in ovo* for 20-24h in a humidified incubator at 38°C.

Quantitative real time RT-PCR

Total RNA from the samples was extracted using a combination of TRIzol reagent (Invitrogen) and RNeasy Mini Kit (QIAGEN) according to the manufacturer's instructions. RNA samples were obtained from freshly isolated 3/4PAR from qE3 (3/4PAR-0h) and from 3/4PAR grown *in vitro* for 48h (3/4PAR-48h). Triplicates of 7 explants per sample were analysed for each condition. After DNAse treatment for 15 min, first-strand cDNA synthesis was performed in a total volume of 20µL, by reverse transcription of 300ng of total RNA using the SuperScript™ III Reverse Transcriptase kit and Oligo $(dT)_{12-18}$ Primer (Invitrogen), according to the manufacturer's instructions. All steps of RNA extraction and cDNA synthesis were performed in a vertical laminar flow hood to avoid contamination. Concentration and purity of both the RNA and cDNA samples were determined using a NanoDrop® ND-1000 Spectrophotometer (Thermo Scientific).

To exclude the amplification of genomic DNA, primers were designed to span introns near the 3'poly-A tail using Primer3 software (Table 1). Quantitative RT-PCR (qRT-PCR) assays were run in a ViiA7™ Fast Real-Time PCR System (Applied Biosystems) in MicroAmp® Optical 384-Well Reaction Plate (Applied Biosystems). Reactions were performed in a final volume of 10µL using 5µl of Power SYBR® Green PCR Master Mix (Applied Biosystems), 0.4µM final concentration of primers and 1µl (up to 1µg) of cDNA. Thermocycling conditions were as follows: an initial denaturation at 50°C for 20sec and 95°C for 10min, followed by 40 cycles at 95°C for 15sec and at 60°C for 1min. To confirm primer specificity, a melting curve was generated at the end of each experiment. Relative quantification of gene expression was determined by the ΔΔCt method (Livak and Schmittgen, 2001) using β-actin (*Actb*) and Hypoxanthine-guanine phosphoribosyltransferase (*Hprt*) as endogenous genes. Three technical replicates were used for each condition.

In situ hybridisation and immunohistochemistry

Quail and chicken embryos, *in vitro* explants and CAM-derived explants were fixed overnight in 4% paraformaldehyde/PBS at 4°C. Samples were then processed for whole-mount *in situ* hybridisation, immunohistochemistry and immunofluorescence.

Whole-mount preparations were hybridised with *Delta1* (Henrique et al., 1995), *Fgf8* (Crossley et al., 1996), *Foxn1* (Neves et al., 2012), *Gata3* (Lilleväli et al., 2007), *Gcm2* (Neves et al., 2012), *Gli1* (Marigo et al., 1996a), *Gli3* (Marigo et al., 1996a), *Hey1* (Leimeister et al., 2000), *Jag1* (Myat at al., 1996), *Lfng* (Aulehla et al., 1999), *Notch1* (Myat at al., 1996), *Shh* (Riddle et al., 1993), *Patched1* (Marigo et al., 1996b) and *Pax1* (Wallin et al., 1996) probes as previously described (Etchevers et al., 2001; Henrique et al., 1995). Paraffin sections of CAM-derived explants grown for 3 days were *in situ* hybridised with *Foxn1* and *Hes5.1* (Fior and Henrique, 2005).

Paraffin sections of explants developed *in ovo* for 10 days were analysed by haematoxylin-eosin staining (H&E) to determine the number, size and morphology of thymic lobes and parathyroid glands formed. Sections of CAM-explants were further treated for immunocytochemistry with the anti-pan [Lu-5] Cytokeratin antibody (Pan CK) (Abcam; for labelling epithelial cells).

Microscopy

H&E and immunohistochemistry images were collected using Software Leica Firewire and Leica DM2500 microscope with Leica DFC420 camera. WM-ISH pictures were taken under a Leica Z6 APO equipped with a Leica DFC490 camera.

Statistical analysis

Means and standard deviations were determined with Microsoft Excel/GraphPad Prism® (version 6.01) software. Two-tailed Student's *t*-tests and Mann-Whitney non-parametric tests were used for the analysis of *in vitro* and *in ovo* assays, respectively. Results were considered significantly different when the *P* value was less than 0.05 ($P< 0.05$).

Results

Notch-target genes Hey1, Hes5.1 and Gata3 are involved in the 3rd and 4th pharyngeal pouches endoderm development.

To investigate the role of Notch signalling during the development of thymus and parathyroids (T/PT) common primordium we analysed the expression of Notch-target genes,

Hey1, *Hes5.1*, *Hes6.1* and *Gata3* (Fang et al., 2007; Naito et al., 2011), within the presumptive territories of these organs (3/4PAR) (Figure 2).

Notch-target gene expression was evaluated during normal development of the 3/4PAR. qE3 3/4PAR was isolated (3/4PAR-0h) and grown *in vitro* for 48h (3/4PAR-48h) (Figure 2A). As depicted in Figure 2B, high levels of *Hey1* and *Gata3* transcripts were detected in freshly isolated tissues and significantly decreased after 48h of culture. A similar trend was observed in in the lowly-expressed transcripts, *Hes5.1* and *Hes6.1*. The reduction of *Hey1* and *Gata3* transcript levels was further supported by *in vivo* gene-expression evaluation at similar developmental time-windows, i.e. qE3 and qE4. *Hey1* transcripts were broadly detected along the endoderm, mesenchyme and ectoderm of the 3/4PAR (Figure 2C and D) whereas *Gata3* expression was restricted to the endoderm of the pouches. At qE3, the strongest *Gata3* hybridisation signals were observed in the tips and anterior domain of the 3PP endoderm (Figure 2E), the T/PT common primordium territory. After 24h of development, *Gata3*-expression domain was confined to a more median/anterior position (Figure 2F), at the parathyroid rudiment territory (Neves et al., 2012). *Gata3* expression was maintained later in the developing parathyroids (Suppl. Fig. 1A). Interestingly, Gata3 has been previously shown to be involved in parathyroid formation (Grigorieva et al., 2010).

Notch signalling was then modulated during common primordium formation (Figure 2A and G-L). 3/4PAR was grown *in vitro* in the presence of three doses of the Notch inhibitor LY-411.575 (Ly), at 50nM, 100nM and 200nM (Figure 2G). A strong and significant reduction of *Hey1* (67%, 77% and 74%) and *Hes5.1* expression (98%, 74% and 92%) was observed in the pharyngeal tissues treated with Ly (Ly-50, Ly-100 and Ly-200, respectively), when compared to control conditions. *Gata3* transcript levels were also diminished (45%, 31% and 29% in Ly-50, Ly-100 and Ly-200, respectively) while no changes were observed for *Hes6.1* expression in either condition. This Notch-target gene belongs to the Hes6 family previously reported to be transcriptionally repressed by Hes5 genes (Fior and Henrique, 2005).

To validate the specificity of Notch signalling inhibition effects, similar *in vitro* assays were performed using three doses (5μM, 10μM and 15μM) of a different Notch inhibitor, Dibenzazepine (DBZ) (Figure 2H). As expected, a strong decrease of *Hey1* (72%, 71% and 66%) and *Hes5.1* (93%, 93% and 98%) transcript levels was accompanied with a less impressive reduction in *Gata3* expression (46%, 38% and 26%) in explants cultured with increasing doses of DBZ. Likewise, the expression levels of *Hes6.1* in DBZ-treated explants were similar to control conditions.

The capacity to inhibit Notch was further confirmed by an *in vivo* approach with the injection of Ly (5-20μM) on the right side of the pharyngeal region of developing embryos. Ly

administration was performed at cE2.5, the developmental stage prior to the formation of T/PT common primordium and to the *in situ* detection of *Gcm2* (Okabe and Graham, 2004). Injected embryos were allowed to develop for 20-24h and then *in situ* analysed for *Hey1* and *Gata3* expression (Figure 2I-L). These genes were selected because of their high expression during *in vitro* development (Figure 2B). Chicken embryos were used in these experiments as some of the probes were inefficient for WM-ISH in quail embryos. In Ly-injected embryos, *Hey1* expression was abolished in all tissues of the pharyngeal region (Figure 2J, n=3/3), while *Gata3* expression was downregulated in the dorsal/tip and anterior domains of common primordium (Figure 2L, n=9/11).

Taken together, our data show that Notch-target genes *Hey1* and *Gata3* may act as positive mediators of Notch activity during the development of the T/PT common primordium.

Notch signalling inhibition promotes the reduction of Foxn1 and Gcm2/Pth expression in the endoderm of the 3rd and 4th pharyngeal pouches.

To investigate the effects of Notch signalling inhibition during common primordium stages, we analysed the transcript levels of the T- and PT-related markers, *Foxn1* (Neves et al., 2012) and *Gcm2/Pth* (Neves et al., 2012; Grevellec et al., 2011) genes, respectively (Figure 3). The expression analysis was expanded to transcription factors known to be involved in the morphogenesis of the pouches and formation of these organs, the *Pax1* and *Fgf8* genes (Dietrich and Gruss, 1995; Wallin et al., 1996; Su et al., 2001; Guo et al., 2011; Frank et al., 2002). *In vitro* and *in vivo* assays were performed as described in the previous section (schematic representation, Figure 3A).

We began by examining the *in vitro* development of pharyngeal tissues (Figure 3B). Predictably, *Foxn1* transcripts were almost undetectable in 3/4PAR-0h but increased 35-fold during 48h culture, confirming thymic epithelium specification during this developmental time-window (Neves et al., 2012). Conversely, the transcription factor *Gcm2* was already strongly expressed in freshly isolated tissues and increased 4-fold in 3/4PAR-48h. In parallel, we observed a striking augmentation of *Pth* expression (986-fold), an indication of parathyroid epithelium differentiation (Günther et al., 2000). Minor changes were globally detected in the expression of *Pax1*, while *Fgf8* transcripts were significantly reduced. A similar trend was observed in the gene expression patterns of *Pax1* and *Fgf8 in situ* at similar developmental time-windows (qE3 and qE4; Figure 3C-F). High levels of *Pax1* expression were observed in the 3/4PP endoderm. The stronger hybridisation signals were confined to the dorsal tip of the pouches (Figure 3C and D), the presumptive territory of the thymic rudiment (Neves et al., 2012). The expression of *Pax1* was maintained in the thymic epithelium at later stages of

development (Suppl. Fig. 1C), as has been observed in mice (Wallin et al, 1996). Faint hybridisation signals of *Fgf8* were observed in the posterior/median domain of the 3/4PP endoderm at qE3 (Figure 3E) and almost disappeared at qE4 (Figure 3F). In short, our *in vitro* system reproduced the normal dynamic of *Foxn1*, *Gcm2*, *Pth*, *Pax1* and *Fgf8* expression in the developing endoderm of the 3/4PP. The *in situ* study also confirmed the restricted expression of *Pax1* and *Fgf8* in the endodermal pouch compartment at these stages of development.

To analyse the effects of Notch inhibition, pharyngeal tissues were treated with Ly (Figure 3G), as described above. When compared to control conditions, a significant reduction of *Foxn1* expression was observed in Ly-derived explants (35%, 56% and 49% in Ly-50, Ly-100 and Ly-200, respectively), suggesting that the abolishment of Notch activity compromises thymic epithelium specification. A significant decrease of *Pax1* expression (46%, 55% and 65%) was also consistently observed with increasing doses of Ly. In addition, Ly-treated tissues showed a reduction of *Gcm2* transcript levels (around 80%), alongside the almost total lack of *Pth* expression (more than 90% reduction), revealing the requirement of Notch signalling activity in the early-stages of parathyroid epithelium differentiation. No significant changes in *Fgf8* expression levels were detected during *in vitro* development.

Similar results were obtained when Notch signalling was abrogated using DBZ (Figure 3H). *Foxn1*, *Gcm2*, *Pth* and *Pax1* transcript levels were significantly reduced in DBZ-treated explants. The expression levels of *Fgf8* were similar in the DBZ and control conditions.

The *in vivo* results (Figure 3A and I-L) supported the *in vitro* effects, as described above. Ly was injected in the 3/4PAR at cE3.5, the corresponding stage to qE3, and allowed to develop for further 20-24h. As previously reported (Neves et al., 2012), *Foxn1*- and *Gcm2*-expression domains were localized in the dorsal-tip (n=4/4; Figure 3I) and median/anterior (n=5/5; Figure 3K) region of the 3/4PP, respectively, in control embryos (Control-DMSO). The expression of *Foxn1* (n=4/4; Figure 3J) and *Gcm2* (n= 5/5; Figure 3L) was strongly diminished in the pouches of Ly-injected embryos. The decrease of *Gcm2* expression was only observed in embryos injected with the highest concentration of Ly (20μM), whereas *Foxn1* expression was reduced even with the lowest dose (5μM). Concordantly, only transcripts of *Gcm2*, and not *Foxn1*, were clearly detected in freshly isolated tissues at qE3 (Figure 3B), the developmental stage similar to the moment of embryo injection.

These data provide evidence that Notch signalling has positive regulatory effects during the development of the T/PT common primordium.

Notch signalling inhibition during early-development of the 3rd and 4th pharyngeal arch region impairs the subsequent formation of parathyroid glands.

We then asked if Notch signalling was required at the T/PT common primordium stage for the respective organ formation. To address this question, Ly-treated tissues were grafted onto CAM and allowed to develop *in ovo* for 10 days (Figure 4A).

We have previously used *in ovo* assays to evaluate the capacity of explants to form organs when grafted onto CAM (Neves et al., 2012). Distinct pharyngeal derived organs displaying normal tissue-tissue interactions were formed in CAM-derived DMSO-free explants (3/4PAR-48h) (Suppl. Fig. 1D-J). These organs were, however, anatomically displaced due to physical constrains during the ectopic growth in CAM. Briefly, chimeric thymus was formed as a result of quail thymic epithelial colonization by lymphoid progenitor cells of donor origin (chicken) (Suppl. Fig. 1F). Thymic lobes showed normal morphological characteristics with discrete cortical and medullary compartments (Suppl. Fig. 1E). Only one third of the lobes were formed per explant (4, n=6), compared with the usual bilateral segmentation of up to 7 thymic lobes per embryo. Regarding the parathyroid glands, each explant showed similar size and number of organs formed (1.7, n=6) when compared to normal embryogenesis (2 parathyroids per embryo). The glands showed normal morphological features with parenchymal cells arranged in clusters, encircled by numerous capillaries and surrounded by a dense and irregular connective tissue capsule (Suppl. Fig. 1H and I).

The ability of the pharyngeal tissues treated with Ly (3/4PAR Ly-200) to form organs when grafted onto CAM was then assessed (Graft-Ly) (Figure 4B-M). The number of thymic lobes formed in Graft-Ly was slightly higher than in control conditions, but with similar sizes (Figure 4B) and normal morphology (Figure 4D and F). These results demonstrated that absence of Notch signals at the common primordium stage was not sufficient to block thymus formation. Moreover, the subsequent development of the thymic rudiment may have been caused, at least partly, by the reactivation of Notch activity in the drug-free CAM environment. When Ly-derived explants were analysed 3 days post-grafting onto CAM strong *Hes5.1* expression was observed, confirming the reactivation of Notch signalling (Figure 4H, n=3/4). Likewise, *Foxn1* expression was detected in thymic rudiments derived from Graft-Ly (Figure 4H´) and Graft-Control (Figure 4G´, n=3/3). Altogether, the data indicate that early-absence of Notch signalling may delay thymic epithelium specification from the T/PT common primordium without blocking it. To further explore the role of Notch signalling at later stages of thymus development, explants were grown in CAM with daily administration of 200nM of Ly. Under these conditions, Notch signalling blocking was not achieved, as assessed by Notch-target gene-expression analysis (data not shown). This was probably due to the inaccessibility and/or inappropriate concentration of Ly. The number, size and morphology of the thymuses formed were similar in CAM-derived explants irrespectively of *in ovo* daily administration of Notch inhibitor (data not shown).

The capacity of *in vitro* Ly-treated pharyngeal tissues to form parathyroids was then evaluated (Figure 4I-M). We observed both fewer and significantly small sized parathyroid glands in Graft-Ly explants (40% less than control) (Figure 4I). These glands also showed poorly developed parenchymal cells clusters (Figure 4K and M). These results demonstrate that Notch signalling inhibition at the T/PT common primordium stage is sufficient to prevent normal parathyroid epithelium differentiation and to irreversibly compromise long-term organ formation.

Having shown parathyroids aplasia/hypoplasia in cultured explants deprived of Notch signals, we asked if Notch regulates cell-proliferation and/or cell-death during common primordium stages. 3/4PAR grown *in vitro* with 200nM of Ly was fixed and analysed *in situ*. Apoptotic and mitotic cells were identified by the presence of Casp3 (Suppl. Fig. 2A and B) and Phos-H3 (Suppl. Fig. 2C and D), at 24h and 48h of development, respectively. The number of $Casp3^{+}$ $E\text{-}Cad^{+}$ cells was similar in 24h-cultured tissues, regardless of the drug treatment (1133±431 and 958±183 apoptotic cells/mm^2 of endodermal tissue in Control- and Ly-derived explants, respectively) (Suppl. Fig. 2A and B). When tissues were analysed after 48h in culture, no differences were observed in the number of Phos-H3 positive nuclei in experimental and control conditions (229±40 and 250±53 mitoses/mm^2 of endodermal tissue in Control- and Ly-derived explants, respectively). Moreover, almost no apoptotic features, characterized by pyknosis, were observed with DAPI staining (Suppl. Fig. 2C and D). Accordingly, similar survival rates were observed in CAM-derived explants [75% (n=6/8) in Graft-Control and 88% (n=8/9) in Graft-Ly], suggesting no involvement of Notch signalling in proliferation/cell death during 3/4PP endoderm development.

Altogether the results indicate that blocking Notch signalling activity during the common primordium stage impairs parathyroid gland formation, possibly by preventing normal epithelium differentiation, without affecting thymus development.

Hedgehog modulates Notch signalling in the developing endoderm of the 3rd and 4th pharyngeal pouches.

Given the role of Notch as a modulator of Hh signalling in the dorso-ventral patterning of the neural tube (Stasiulewicz et al., 2015), we further investigated if Hh signalling could be modulated by Notch during T/PT common primordium formation.

We started by studying the expression of distinct Hh-related genes in pharyngeal tissues (Figure 5A-G). The expression of *Patched1* (Hh receptor), *Shh* (Hh ligand), *Gli1* and *Gli3* (Hh-target genes) was analysed during *in vitro* (Figure 5A) and *in vivo* (Figure 5B-G) development, as described above. *Shh* was the most highly expressed Hh-related gene in the developing

3/4PAR (Figure 5A). Its expression was confined to the endodermal territory of the central pharynx, excluding the 3/4PP (data not shown). The transcript levels of *Patched1* were maintained during 48h of culture and its hybridisation signals were faint in all pharyngeal tissues (Figure 5B and E). Interestingly, *Gli1* and *Gli3* transcripts were significantly reduced during *in vitro* development. The *in situ* analysis of these genes revealed hybridisation signals of *Gli1* (Figure 5C and F) and *Gli3* (Figure 5D and G) along the endoderm, mesenchyme and ectoderm of the 3/4PAR. However, *Gli3* expression was more evident in the anterior/dorsal tip- (Figure 5D) and posterior/dorsal tip-domains (Figure 5G) of the 3PP endoderm, at qE3 and qE4, respectively.

Having demonstrated which genes are involved in the activation of Hh in the 3/4PAR, we asked if blocking Notch activity could interfere with Hh signalling. The expression of Hh-related genes was quantified in 3/4PAR grown *in vitro* for 48h in the presence of either Notch inhibitor. When compared to control conditions, no differences were observed in the transcript levels of the four genes in Ly- or DBZ-treated tissues (Figure 5H and I). These *in vitro* effects were confirmed by a Hh-related gene-expression analysis of embryos that had Notch signals blocked at similar developmental-time windows. No obvious changes in *Patched1*, *Gli1* and *Gli3* expression were observed in Ly-injected embryos, when compared to control embryos (Suppl. Fig. 3).

To clarify the interactions between the Notch and Hh pathways, we then questioned if Hh activity could modulate Notch signalling during common primordium formation. Pharyngeal tissues were treated with Cyclopamine (Cyc), a well-described teratogen known to inhibit Hh signal transduction by binding to the heptahelical bundle of Smoothened (Chen et al., 2002). In parallel, another Hh inhibitor Vismodegib (Vis) was used to validate the *in vitro* Hh inhibitory effects. The expression of Notch-target genes was then analysed in explants grown in the presence of these inhibitors to evaluate the capacity of Hh activity to modulate Notch during common primordium formation (Figure 5J and K). Explants grown in the presence of Cyc or Vis showed a significant reduction of *Hey1* (63% and 29%, respectively) and *Hes5.1* (79% and 60%, respectively) transcript levels, suggesting Notch signalling modulation by Hh during this developmental time-window. Concordantly, no changes were observed in the expression of *Hes6.1* and *Gata3*.

The block of Hh signalling was confirmed by the strong reduction of *Patched1* expression (80%) in tissues grown with either Hh inhibitor (Figure 5K), as previously described (Grevellec et al., 2011; Cordero et al., 2004). A significant reduction of *Shh* transcripts was also detected in Cyc-treated explants, as has been reported in other developmental contexts (Cordero et al., 2004). The expression levels of *Gli1* and *Gli3* were unchanged in both experimental conditions.

Finally, functional readouts of *in vitro* Hh inhibition with Cyc were evaluated (Suppl. Fig. 4). Consistent with results reported in the $Shh^{-/-}$ mice phenotype (Moore-Scott and Manley, 2005), a significant increase in *Foxn1* expression was accompanied with a reduction of the parathyroid-markers, *Gcm2* and *Pth*, in Cyc-treated explants (Suppl. Fig. 4A). The moderate reduction of *Gcm2* transcripts, in contrast with its absence in the mutant mice, is in accordance with a less responsive *Gcm2*-expression domain to Hh at these stages of development (Grevellec et al., 2011). Moreover, pharyngeal tissues with compromised Hh activity showed massive apoptosis, disruption of epithelial integrity (Suppl. Fig. 4B´and C´) and low survival rates when grafted onto the CAM, resulting in thymic hypoplasia and abnormal parathyroid formation (Suppl. Fig. 4E-I´). The results are consistent with previous reports describing the role of Hh in the formation of pharyngeal endoderm-derived organs (Moore-Scott and Manley, 2005; Grevellec et al., 2011; Shah et al., 2004; Outram et al., 2009).

Together, the data suggest a fine-tuning modulation of Notch and Hh pathways during T/PT common primordium formation. Importantly, Hh signalling may regulate Notch activity during this developmental time-window.

Hedgehog modulates Notch signalling in distinct domains of the developing endoderm of the 3rd and 4th pharyngeal pouches.

As shown above, Hh regulates the expression of Notch-target genes in cultured tissues. We therefore carried out *in vivo* modulation of Hh activity during the development of T/PT common primordium. Beads soaked with Cyc (6mM) were placed in the lumen of the pharynx through the second cleft and sited near the 3/4PP at cE2.5 and qE3. After 20-24h of development, embryos were fixed and analysed by WM-ISH for Notch-target genes and organ epithelial markers (Figure 6).

Embryos developed with low Hh activity in the pharyngeal region showed a reduction in *Gata3* expression in the anterior/median territory of the 3PP endoderm (Figure 6E, n=4/5), when compared with control embryos (Figure 6A, n=5/5). In the same pouch region, we observed the loss of *Gcm2* expression (Figure 6F, n=4/5), an expected result considering that $Shh^{-/-}$ mice have no *Gcm2* expression in the presumptive territory of the parathyroids (Moore-Scott and Manley, 2005). These results suggested that Hh activity positively regulates Gata3/Notch signals in the Gcm2/parathyroid-fated domain of the 3/4PP endoderm. However, embryos with Cyc-soaked beads (Cyc-beads) showed the maintenance of *Gata3* expression in the dorsal tip of the 3PP, the presumptive thymic domain (Figure 6E). At later stages, low Hh activity in the pharyngeal region led to a decrease of *Gata3* expression in the 4PP endoderm of qE3 (a similar stage to cE3.5, Figure 6J) embryos (Figure 6G, n=3/3). This effect recapitulates

the one observed in the 3PP at an earlier stage of development (cE2.5). This dynamic spatial and temporal action of Hh signalling has already been described for the modulation of *Gcm2* expression during PP development (Grevellec et al., 2011).

To further investigate downstream targets of Hh signalling in the presumptive thymic rudiment, we screened for the expression of other Notch-related genes in 3/4PP endoderm. Several genes were studied and their expression patterns were unaltered or inconsistently modified when Hh signalling was impaired (Suppl. Fig. 5A-F). Only *Lfng*, a Notch modulator, showed robust modified expression in these conditions. *Lfng* is normally expressed in the posterior/median territory of the 3PP endoderm (Figure 6D, n=4/4), the territory excluded from the T/PT common primordium, and in mesenchymal cells. In the absence of Hh signals, its expression was downregulated in the pouch and in some neighbouring cells (Figure 6H, n=4/4). Lfng is known to inhibit Jag1-mediated signalling and to potentiate Notch1 activation via the Delta1 ligand (Hicks et al., 2000). In cE3, faint expression of *Notch1* (Figure 6I) and *Delta1* (Figure 6K) was observed in the endoderm and neighbouring cells of the 3PP. The expression of *Jag1* (Figure 6L) appeared more restricted to the anterior/median domain of the 3PP. The data indicate a preferential activation of Notch via Lfng/Delta1 in the posterior/median domain of the pouches.

Having in mind that the posterior boundary of Foxn1/thymus-fated domain is the *Lfng*-expression domain, we questioned if the territory of the former could be altered when Hh signalling was abolished. When compared to controls (Figure 6M, n=7/7), qE3 embryos with Cyc-beads presented an enlarged *Foxn1*-expression domain with stronger hybridisation signals (Figure 6N, n=4/6). The expansion of the Foxn1/thymus-fated domain was from the dorsal tip to a more posterior/median region of the pouch. This territory partially overlapped with the *Lfng*-expression domain, which in turn was prevented in the absence of Hh. These results thus suggest that Lfng/Notch activity defines the posterior boundary of the Foxn1/thymus-fated domain, in an Hh-dependent manner.

Notably, an enriched expression of *Foxn1* was observed in the 2PP endoderm (Figure 6N), suggesting that Hh signalling prevents the Foxn1/thymus-fated domain in the most anterior pouches. Similar ectopic and abnormal *Gcm2* expression in the 2PP was previously reported as a result of Hh inhibition (Grevellec et al., 2011).

Discussion

In avians, as in mammals, the thymus and parathyroids epithelia derive from a common endodermal primordium of the pharyngeal pouches. This process involves the patterning of the pouches followed by rudiment specification. In this study, we propose that the temporal and

spatial dynamics of the pharyngeal morphogenesis are regulated by Notch and Hh signals during the development of the T/PT common primordium and the formation of thymic and parathyroid rudiments.

Thymus and parathyroids common primordium

In avians, as opposed to mice, the thymus and parathyroid epithelia derive not from one (3PP) but from two sequentially developing pharyngeal pouches, the 3PP and 4PP. Consistent with the temporal gap of 12h to 24h between the formation of the two pouches, a delay in the expression of several transcriptional regulators known to be involved in PP patterning and early-formation of these organs has also been observed (Manley and Condie, 2010). For example, *Gcm2* expression in the anterior domain of the 3PP was first reported at HH18 (cE3; qE2.5), prior to the formation of the 4PP. Only at HH22 (cE4; qE3) was the expression of *Gcm2* observed in the 4PP (Okabe and Graham, 2004). To overcome this complexity we opted to perform the *in vitro* studies at qE3 stage when both pouches are already formed.

We observed a consistent impairment in the development of the T/PT common primordium when Notch signalling was *in vitro* and *in vivo* inhibited (schematic representation in Figure 7A). The expression of thymic and parathyroid markers (*Foxn1* and *Gcm2/Pth*) was strikingly decreased. These effects were accompanied with the reduction of *Gata3*, suggesting that this Notch-target is a downstream mediator of Notch activity during common primordium development. In agreement, heterozygous mice mutants for Gata3 have smaller T/PT common primordium with fewer cells expressing *Gcm2* (Grigorieva et al., 2010).

When Hes1, another Notch-target, was deleted in neural crest cells, there was aplasia/hypoplasia of these organs, stressing the importance of driving specific Notch signals into distinct tissues during early stages of thymic and parathyroid formation (Kameda et al., 2013). We have previously developed an *in vitro* experimental system with the heterospecific association of quail and chicken tissues, which has allowed us to study epithelial-mesenchymal interactions during thymus and parathyroid organogenesis (Neves et al., 2012). Insufficient information on quail and chicken genetic sequences has been a limiting step for discriminating tissues of different origin by qRT-PCR assays. As a consequence, the complete distinction of the endodermal and mesenchymal specific functions during organ formation, particularly important in a cell-cell contact signalling activation like in the Notch pathway, could not be fully addressed in this study.

We identified a new domain in the 3PP at qE3 (cE3.5), excluded from the common primordium, in which the Notch-modulator *Lfng*, and also *Fgf8* were expressed. The reduction of *Lfng* and *Fgf8* (Suppl. Fig. 4A) in the absence of Hh suggests that this domain may be

involved in the regulation of T/PT common primordium development, in an Hh-dependent manner. These data, though limited, suggests a putative Shh-Fgf8-Lfng network, involving distinct signalling centres located in the endoderm of the pharynx and within the pouches. In other biological contexts, Lfng is known to respond to Fgf8 signals (Shifley et al., 2008). On the other hand, Fgf8 has been shown to respond to Shh produced by the pharyngeal endoderm during arch patterning (Haworth et al., 2007). And in the developing 3PP, a hyper-responsiveness to Fgf8 alters, at least in part, the initiation of parathyroid- and thymus-fated markers (Gardiner et al., 2012).

The endoderm of the pharynx is indeed the main source of Hh signals, via Shh secretion, during the development of the T/PT common primordium (Figure 7B). The median/anterior and median/posterior territories of the developing pouches are closer to the source of Hh, as opposed to the tips, which will grow apart to more dorsal and ventral positions. At qE3, expression of various Notch-related genes is distributed along the pouches. The median/anterior region and tips of the pouch originate a *Gata3*-expression domain while the median/posterior territory gives rise to the *Lfng*-expression domain. The restricted median/anterior domain of *Gata3* also co-expresses *Gcm2*. As development proceeds, the *Gata3*/*Gcm2* domain starts to express *Pth* and becomes more restricted to a smaller central territory of the anterior/median region of the pouch (Figure 7A), originating the parathyroid rudiment at qE4 (Neves et al., 2012).

When Hh signals were abolished in the pharynx, downregulation of *Gata3*/*Gcm2* and *Lfng* expression was observed, indicating that the median domains of the pouches are positively regulated by Hh signalling. In contrast, the expression of *Gata3* was maintained at the tips of the pouches, suggesting that there are Gata3/Notch signals in the common primordium that respond differently to Hh (schematic representations in Figure 7C). It is therefore conceivable that during the specification of the rudiments, the parathyroid-fated domain is more sensitive to Hh signalling, while the thymus-fated domain is unresponsive to Hh.

Overtime, the source of Shh gets further away and overall the pouches become less sensitive to Hh. In fact, the upregulation of *Gcm2* was reported to correlate with the loss of Hh receptor *Patched1* during 3PP development in mice (Grevellec et al., 2011).

Parathyroid rudiment

The specification of the parathyroid rudiment is known to be dependent on *Gcm2* transcriptional activation. Deficiency of Gcm2 in mice leads to the absence of parathyroid glands without affecting thymus formation (Liu et al., 2007). Notch-target Gata3 (Fang et al., 2007; Naito et al., 2011) is one of the upstream regulators of Gcm2, as $Gata3^{-/-}$ mice showed no *Gcm2* expression and no gland formation (Grigorieva et al., 2010). In this investigation, the

decreased expression of *Gata3* was accompanied by a sharp reduction of *Gcm2* in the absence of Notch, demonstrating a Notch signalling activation requirement, via Gata3, for parathyroid epithelium differentiation. Evidence supporting this hypothesis was the loss of *Pth* expression and abnormal parathyroid formation, when common primordium was grown in the absence of Notch activity. It has been recently shown in mice that Gata3 cooperates with Gcm2 to activate *Pth* expression (Han et al., 2015).

Apart from a possible role in epithelium differentiation, Gata3/Notch signals may also regulate cell survival in the parathyroid rudiment. The impairment of Gcm2/Gata3-Notch signals results in the reduced number and size of the parathyroids, in accordance with the mouse model where parathyroid precursors undergo rapid apoptosis in the absence of Gcm2 (Lui et al., 2007). Although no differences were detected in the number of proliferating or apoptotic cells in the developing pharyngeal endoderm treated with Ly, we cannot exclude the role of Notch in these biological processes. *In situ* analysis showed small clusters of apoptotic cells on the endoderm grown *in vitro* for 24h (not shown). This suggests well-defined domains with a tight regulation of cell numbers that may correspond to organ rudiments, that is, the parathyroid glands. We also postulate that these untraced apoptotic events may occur even earlier during *in vitro* development.

During the course of our study we further attempted to identify the Notch ligands involved in PT rudiment formation. Only *Jag1* was confined to the median/anterior territory of the pouches at cE3, overlapping with the Gcm2/parathyroid-fated domain. The capacity of *Jag1*-expressing cells to define boundaries by lateral inhibition has been reported in other developmental processes (Kiernan, 2013). In this study, the *Jag1*-expression domain, as opposed to the Gata3/Gcm2/parathyroid-fated domain, was not altered when the pharyngeal source of Hh was abolished (Suppl. Fig. 5B), suggesting that Jag1 defines the boundary of the rudiment independent of Hh. It may be that parathyroid cell-fate specification, accompanied by the definition of the boundary of the rudiments, occurs earlier in development. In agreement with this, the location of the parathyroid dorsal boundary appears to be unchanged when Gcm2/Pth expression is lost.

Nevertheless, the theory that there is positive regulation of Hh in settling the Gata3/Gcm2/parathyroid-fated domain is supported by the abnormal morphology and size of the glands in the absence of Hh signalling.

Thymic rudiment

The individual thymic rudiment was previously identified by the *Foxn1*-expression domain in the dorsal tip of the pouches at qE4 (Neves et al., 2012). In this work we show that

Foxn1 expression was strongly reduced when Notch signalling was impaired. The early downregulation of *Foxn1* could however be reversed by subsequent restitution of Notch signalling activity in the thymic rudiment.

Notch signalling is known to play a unique function in the control of hair follicle differentiation by modulation of *Foxn1* (Hu et al., 2010). Although hair is an epidermal appendage that arose after the last shared common ancestor between mammals and birds, embryonic chicken feathers and nails also express *Foxn1*, demonstrating the conservation of these developmental processes during evolution (Darnell et al., 2014). In addition, nude mice ($Foxn1^{-/-}$) have two major defects, abnormal hair growth and defective development of the thymic epithelium (Nehls et al., 1996; Blackburn et al., 1996; Bleul et al., 2006), suggesting a common Notch-Foxn1 pathway in both developmental processes.

The Notch-target gene Gata3 may be one of the upstream regulators of Foxn1, since *Gata3* is expressed in the dorsal tip of the 3/4PP endoderm during T/PT common primordium formation. At this developmental stage, *Gata3* in the prospective thymic rudiment is modulated by Notch (schematic representation in Figure 7C).

When Hh signalling was blocked, we observed an expansion of the Foxn1/thymus-fated domain to a more median/posterior region, at the expense of the loss of *Lfng*–expression domain (Figure 7C). The capacity of the thymic rudiment to expand posteriorly suggests some degree of cell-fate plasticity of endodermal cells in the posterior/median domain of the pouch. Together with *Lfng*, the only Notch ligand faintly expressed in the median/posterior territory of the pouches was *Delta1*. Lfng typically enhances Notch activation by ligands belonging to the Delta family and reduces Notch activation by Jagged family ligands (reviewed in Stanley and Okajima, 2010). This suggests that the posterior thymic boundary is determined by a lateral inhibition mechanism via Delta1. In the absence of Hh signals in the pharyngeal region, the disappearance of the *Lfng*-expression domain may result in reduced Delta1 activity and boundary displacement. Specifically, a reduction of the Delta1 signalling strength gradient may result in an augmentation of the posterior thymic rudiment territory. Here, we report the previously unreported regulation of the posterior boundary of thymic rudiment by Notch signalling via Lfng, in an Hh-dependent manner (Figure 7C).

Another Notch-target gene, *Hey1*, was markedly reduced when Notch activity was blocked in the pharyngeal tissues. Although *Hey1* expression was not restricted to the endoderm of the pouches, our data suggest its involvement in the primordium development. In agreement, a recent report showed *Hey1* expression in the thymic epithelium of mice (Subhan et al., 2013).

The transcription factor Pax1, important for thymus (Dietrich and Gruss, 1995; Wallin et al., 1996) and parathyroid (Su et al, 2001) formation, was also downregulated when Notch

signalling was inhibited, suggesting that Notch may act upstream of Pax1 during T/PT common primordium development. Taking into account that *Pax1* is expressed very early in pouch formation (not shown) and during thymic epithelium differentiation; it is therefore conceivable that distinct mechanisms may positively regulate Pax1, from pharyngeal pouch morphogenesis to thymus organogenesis. A biphasic role in these distinct windows of development was recently described for the activity of another transcription factor, the Tbx1 gene (Reeh et al., 2014).

In conclusion, our work shows that Notch signalling is crucial for T/PT common primordium development and parathyroid formation, in an Hh-dependent manner. Finally, we conclude that, despite the evolutionary distance, the regulatory mechanisms controlling the formation of these organs appear to be conserved in avians and mammals.

Conflicts of interest

The authors declare no conflict of interests.

Acknowledgments

The authors are grateful to Domingos Henrique, Joaquin Rodriguez Leon, Solveig Thorsteinsdottir and Kim Dale for reagents, to Sérgio Dias for helpful discussions and to Interaves Portugal for contributing with quail fertilised eggs. This work was supported by Fundação para a Ciência e para a Tecnologia (FCT), project PTDC/SAU-BID/115264/2009. M. Figueiredo received two research fellowships from FCT.

References

Aulehla A, Johnson RL. 1999. Dynamic expression of lunatic fringe suggests a link between notch signaling and an autonomous cellular oscillator driving somite segmentation. *Dev Biol.* **207**:49-61.

Blackburn CC, Augustine CL, Li R, Harvey RP, Malin MA, Boyd RL, Miller JF, Morahan G. 1996. The nu gene acts cell-autonomously and is required for differentiation of thymic epithelial progenitors. *Proc. Natl. Acad. Sci. U.S.A.* **93**: 5742-6.

Bleul CC, Corbeaux T, Reuter A, Fisch P, Mönting JS, Boehm T. 2006. Formation of a functional thymus initiated by a postnatal epithelial progenitor cell. *Nature* **441**:992-6.

Chen JK, Taipale J, Cooper MK, Beachy PA. 2002. Inhibition of Hedgehog signaling by direct binding of cyclopamine to Smoothened. *Genes Dev.* **16**:2743–8.

Cordero D, Marcucio R, Hu D, Gaffield W, Tapadia M, Helms JA. 2004. Temporal perturbations in sonic hedgehog signaling elicit the spectrum of holoprosencephaly phenotypes. *J Clin Invest.* **114**:485-94.

Crossley PH, Minowada G, MacArthur CA, Martin GR. 1996. Roles for FGF8 in the induction, initiation, and maintenance of chick limb development. *Cell* **84**:127-36.

Darnell DK, Zhang LS, Hannenhalli S, Yaklichkin SY. 2014. Developmental expression of chicken FOXN1 and putative target genes during feather development. *Int J Dev Biol*. **58**:57-64. doi: 10.1387/ijdb.130023sy.

Dietrich S, Gruss P. 1995. Undulated phenotypes suggest a role of Pax-1 for the development of vertebral and extravertebral structures. *Dev Biol.* **167**:529-48.

Dorsch M, Zheng G, Yowe D, Rao P, Wang Y, Shen Q, Murphy C, Xiong X, Shi Q, Gutierrez-Ramos JC, Fraser C, Villeval JL. 2002. Ectopic expression of Delta4 impairs hematopoietic development and leads to lymphoproliferative disease. *Blood* **100**:2046–55.

Etchevers, H.C., Vincent, C., Le Douarin, N.M., Couly, G.F., 2001. The cephalic neural crest provides pericytes and smooth muscle cells to all blood vessels of the face and forebrain. *Development* **128**:1059–1168.

Fang TC, Yashiro-Ohtani Y, Del Bianco C, Knoblock DM, Blacklow SC, Pear WS. 2007. Notch directly regulates Gata3 expression during T helper 2 cell differentiation. *Immunity.* **27**:100-10.

Farley AM, Morris LX, Vroegindeweij E, Depreter ML, Vaidya H, Stenhouse FH, Tomlinson SR, Anderson RA, Cupedo T, Cornelissen JJ, Blackburn CC. 2013. Dynamics of thymus organogenesis and colonization in early human development. *Development*. **140**: 2015-26. doi: 10.1242/dev.087320.

Fior R, Henrique D. 2005. A novel hes5/hes6 circuitry of negative regulation controls Notch activity during neurogenesis. *Dev Biol* **281**:318-333.

Frank DU, Fotheringham LK, Brewer JA, Muglia LJ, Tristani-Firouzi M, Capecchi MR, Moon AM. 2002. An Fgf8 mouse mutant phenocopies human 22q11 deletion syndrome. *Development* **129**:4591-603.

Gardiner JR, Jackson AL, Gordon J, Lickert H, Manley NR, Basson MA. 2012. Localised inhibition of FGF signalling in the third pharyngeal pouch is required for normal thymus and parathyroid organogenesis. *Development* **139**:3456-66. doi:10.1242/dev.079400.

Gordon J, Bennett AR, Blackburn CC, Manley NR. 2001. Gcm2 and Foxn1 mark early parathyroid- and thymus-specific domains in the developing third pharyngeal pouch. *Mech Dev.* **103**:141-3.

Grigorieva IV, Mirczuk S, Gaynor KU, Nesbit MA, Grigorieva EF, Wei Q, Ali A, Fairclough RJ, Stacey JM, Stechman MJ, Mihai R, Kurek D, Fraser WD, Hough T, Condie BG, Manley N, Grosveld F, Thakker RV. 2010. Gata3-deficient mice develop parathyroid abnormalities due to dysregulation of the parathyroid-specific transcription factor Gcm2. *J Clin Invest.* **120**:2144-55. doi: 10.1172/JCI42021.

Grevellec A, Graham A, Tucker AS. 2011. Shh signalling restricts the expression of Gcm2 and controls the position of the developing parathyroids. *Dev Biol.* **353**:194-205. doi: 10.1016/j.ydbio.2011.02.012.

Grevellec A, Tucker AS. 2010. The pharyngeal pouches and clefts: Development, evolution, structure and derivatives. *Semin Cell Dev Biol.* **21**:325-332. doi: 10.1016/j.semcdb.2010.01.022.

Günther T, Chen ZF, Kim J, Priemel M, Rueger JM, Amling M, Moseley JM, Martin TJ, Anderson DJ, Karsenty G. 2000. Genetic ablation of parathyroid glands reveals another source of parathyroid hormone. *Nature* **406**:199-203.

Guo C, Sun Y, Zhou B, Adam RM, Li X, Pu WT, Morrow BE, Moon A, Li X. 2011. A Tbx1-Six1/Eya1-Fgf8 genetic pathway controls mammalian cardiovascular and craniofacial morphogenesis. *J Clin Invest.* **121**:1585-95. doi: 10.1172/JCI44630.

Han SI, Tsunekage Y, Kataoka K. 2015. Gata3 cooperates with Gcm2 and MafB to activate parathyroid hormone gene expression by interacting with SP1. *Mol Cell Endocrinol.* **411**:113-20. doi: 10.1016/j.mce.2015.04.018.

Haworth KE, Wilson JM, Grevellec A, Cobourne MT, Healy C, Helms JA, Sharpe PT, Tucker AS. 2007. Sonic hedgehog in the pharyngeal endoderm controls arch pattern via regulation of Fgf8 in head ectoderm. *Dev Biol.* **303**:244-58.

Henrique D, Adam J, Myat A, Chitnis A, Lewis J, Ish-Horowicz D. 1995. Expression of a Delta homologue in prospective neurons in the chick. *Nature* **375**:787–790.

Hicks C, Johnston SH, diSibio G, Collazo A, Vogt TF, Weinmaster G. 2000. Fringe differentially modulates Jagged1 and Delta1 signalling through Notch1 and Notch2. *Nat Cell Biol.* **2**:515-20.

Hu B, Lefort K, Qiu W, Nguyen BC, Rajaram RD, Castillo E, He F, Chen Y, Angel P, Brisken C, Dotto GP. 2010. Control of hair follicle cell fate by underlying mesenchyme through a CSL-Wnt5a-FoxN1 regulatory axis. *Genes Dev.* **24**:1519-32. doi: 10.1101/gad.1886910.

Jaleco AC, Neves H, Hooijberg E, Gameiro P, Clode N, Haury M, Henrique D, Parreira L. 2001. Differential effects of Notch ligands Delta-1 and Jagged-1 in human lymphoid differentiation. *J Exp Med.* **194**:991-1002.

Jiang R, Lan Y, Chapman HD, Shawber C, Norton CR, et al. 1998. Defects in limb, craniofacial, and thymic development in Jagged2 mutant mice. *Genes Dev.* **12**:1046–57.

Lai EC. 2004. Notch signaling: control of cell communication and cell fate. *Development* **131**:965-973.

Lawson ND, Vogel AM, Weinstein BM. 2002. sonic hedgehog and vascular endothelial growth factor act upstream of the Notch pathway during arterial endothelial differentiation. *Dev Cell* **3**:127-36.

Leimeister C, Dale K, Fischer A, Klamt B, Hrabe de Angelis M, Radtke F, McGrew MJ, Pourquié O, Gessler M. 2000. Oscillating expression of c-Hey2 in the presomitic mesoderm suggests that the segmentation clock may use combinatorial signalling through multiple interacting bHLH factors. *Dev Biol.* **227**:91-103.

Lewis J. 1998. Notch signalling and the control of cell fate choices in vertebrates. *Semin Cell Dev Biol.* **9**:583-589.

Lilleväli K, Haugas M, Pituello F, Salminen M. 2007. Comparative analysis of Gata3 and Gata2 expression during chicken inner ear development. *Dev Dyn.* **236**:306-13.

Liu Z, Yu S, Manley NR. 2007. Gcm2 is required for the differentiation and survival of parathyroid precursor cells in the parathyroid/thymus primordia. *Dev. Biol.* **305**:333-346.

Livak KJ, Schmittgen TD. 2001. Analysis of relative gene expression data using real-time quantitative PCR and the 2(-Delta Delta C(T)) Method. *Methods* **25**:402-408.

Manley NR, Condie BG. 2010. Transcriptional regulation of thymus organogenesis and thymic epithelial cell differentiation. *Prog Mol Biol Transl Sci.* **92**:103-20. doi: 10.1016/S1877-1173(10)92005-X.

Marigo V, Johnson RL, Vortkamp A, Tabin CJ. 1996. Sonic hedgehog differentially regulates expression of GLI and GLI3 during limb development. *Dev Biol*. 180:273-83.

Marigo V, Scott MP, Johnson RL, Goodrich LV, Tabin CJ. 1996. Conservation in hedgehog signaling: induction of a chicken patched homolog by Sonic hedgehog in the developing limb. Development. 122:1225-33.

McGlinn E, van Bueren KL, Fiorenza S, Mo R, Poh AM, Forrest A, Soares MB, Bonaldo Mde F, Grimmond S, Hui CC, Wainwright B, Wicking C. 2005. Pax9 and Jagged1 act downstream of Gli3 in vertebrate limb development. *Mech Dev.* **122**:1218-33.

Moore-Scott BA, Manley NR. 2005. Differential expression of Sonic hedgehog along the anterior-posterior axis regulates patterning of pharyngeal pouch endoderm and pharyngeal endoderm-derived organs. *Dev Biol.* **278** :323-35.

Myat A, Henrique D, Ish-Horowicz D, Lewis J. 1996. A chick homologue of Serrate and its relationship with Notch and Delta homologues during central neurogenesis. *Dev. Biol.* **174**: 233-247.

Naito T, Tanaka H, Naoe Y, Taniuchi I. 2011. Transcriptional control of T-cell development. *Int Immunol.* **23**:661-8. doi: 10.1093/intimm/dxr078.

Nehls M, Kyewski B, Messerle M, Waldschütz R, Schüddekopf K, Smith AJ, Boehm T. 1996. Two genetically separable steps in the differentiation of thymic epithelium. *Science* **272**:886-9.

Neves H, Dupin E, Parreira L, Le Douarin NM. 2012. Modulation of Bmp4 signalling in the epithelial-mesenchymal interactions that take place in early thymus and parathyroid development in avian embryos. *Dev Biol.* **361**:208-19. doi: 10.1016/j.ydbio.2011.10.022.

Neves, H and Zilhão R. 2014. Development of Parathyroid Glands and C-Cells. In: Ashford M, Editor. *Parathyroid Glands: Regulation, Role in Human Disease and Indications for Surgery.* Nova Science Publishers. p1-34.

Okabe M, Graham A. 2004. The origin of the parathyroid gland. *Proc. Natl. Acad. Sci. U.S.A.* **101**:17716–9.

Outram SV, Hager-Theodorides AL, Shah DK, Rowbotham NJ, Drakopoulou E, Ross SE, Lanske B, Dessens JT, Crompton T. 2009. Indian hedgehog (Ihh) both promotes and restricts thymocyte differentiation. *Blood.* **113**:2217-28. doi: 10.1182/blood-2008-03-144840.

Potts JT. 2005. Parathyroid hormone: past and present. *J Endocrinol.* **187**:311–325.

Pui, J.C., D. Allman, L. Xu, S. DeRoco, F.G. Karnell, S., Bakkour, J.Y. Lee, T. Kadesch, R.R. Hardy, J.C. Aster, and W.S. Pear. 1999. Notch1 expression in early lymphopoiesis influences B versus T lineage determination. *Immunity.* **11**:299–308.

Kameda Y, Saitoh T, Nemoto N, Katoh T, Iseki S, Fujimura T. 2013. Hes1 is required for the development of pharyngeal organs and survival of neural crest-derived mesenchymal cells in pharyngeal arches. *Cell Tissue Res.* **353**:9-25. doi: 10.1007/s00441-013-1649-z.

Kiernan AE. 2013. Notch signaling during cell fate determination in the inner ear. *Semin Cell Dev Biol.* **24**:470-9. doi: 10.1016/j.semcdb.2013.04.002.

Radtke F, Wilson A, Stark G, Bauer M, van Meerwijk J, MacDonald HR, Aguet M. 1999. Deficient T cell fate specification in mice with an induced inactivation of Notch1. *Immunity* **10**:547-58.

Reeh KA, Cardenas KT, Bain VE, Liu Z, Laurent M, Manley NR, Richie ER. 2014. Ectopic TBX1 suppresses thymic epithelial cell differentiation and proliferation during thymus organogenesis. *Development* **141**:2950-8. doi: 10.1242/dev.111641.

Riddle RD, Johnson RL, Laufer E, Tabin C. 1993. Sonic hedgehog mediates the polarizing activity of the ZPA. *Cell* **75**:1401-16.

Rodewald HR. 2008. Thymus organogenesis. *Annu Rev Immunol.* **26**: 355-88.

Shah DK, Hager-Theodorides AL, Outram SV, Ross SE, Varas A, Crompton T. 2004. Reduced thymocyte development in sonic hedgehog knockout embryos. *J Immunol.* **172**:2296-306.

Shifley ET, Vanhorn KM, Perez-Balaguer A, Franklin JD, Weinstein M, Cole SE. 2008. Oscillatory lunatic fringe activity is crucial for segmentation of the anterior but not posterior skeleton. *Development* **135**:899-908. doi: 10.1242/dev.006742.

Stanley P, Okajima T.2010. Roles of glycosylation in Notch signaling. *Curr Top Dev Biol.* **92**:131-64. doi: 10.1016/S0070-2153(10)92004-8.

Stasiulewicz M, Gray SD, Mastromina I, Silva JC, Björklund M, Seymour PA, Booth D, Thompson C, Green RJ, Hall EA, Serup P, Dale JK. 2015. A conserved role for Notch signaling in priming the cellular response to Shh through ciliary localisation of the key Shh transducer Smo. *Development* **142**:2291-303. doi: 10.1242/dev.125237.

Su D, Ellis S, Napier A, Lee K, Manley NR. 2001. Hoxa3 and pax1 regulate epithelial cell death and proliferation during thymus and parathyroid organogenesis. *Dev Biol.* **236**:316-29.

Subhan F, Yoon TD, Choi HJ, Muhammad I, Lee J, Hong C, Oh SO, Baek SY, Kim BS, Yoon S. 2013. Epidermal growth factor-like domain 8 inhibits the survival and proliferation of mouse thymocytes. *Int J Mol Med.* **32**:952-8. doi:10.3892/ijmm.2013.1448.

Tomita K, Hattori M, Nakamura E, Nakanishi S, Minato N, Kageyama R. 1999. The bHLH gene Hes1 is essential for expansion of early T cell precursors. *Genes Dev.* **13**:1203-1210.

van Bueren KL, Papangeli I, Rochais F, Pearce K, Roberts C, Calmont A, Szumska D, Kelly RG, Bhattacharya S, Scambler PJ. 2010. Hes1 expression is reduced in Tbx1 null cells and is required for the development of structures affected in 22q11 deletion syndrome. *Dev Biol.* **340**: 369-80. doi:10.1016/j.ydbio.2010.01.020.

Wallin J, Eibel H, Neubüser A, Wilting J, Koseki H, Balling R. 1996. Pax1 is expressed during development of the thymus epithelium and is required for normal T-cell maturation. *Development* **122**:23-30.

Figure Legends

Figure 1. Schematic representation of *in vitro* and *in ovo* experimental design. Sequential mechanical isolation steps of the 3/4PAR (A-C). Ventral (D) and Dorsal (E) views of the isolated 3/4PAR. Schematic representations of the transversal section of the embryo at the region of interest (F) and of the experimental design (G). PAR, pharyngeal arch region.

Figure 2. Notch-target genes are involved in T/PT common primordium formation. Timeline of *in vitro* and *in vivo* assays in chicken and quail development (A). *In vitro* (B) and *in vivo* (C-F) expression of Notch-target genes in the 3/4PAR. Isolated 3/4PAR at qE3 was grown *in vitro* for 48h. The expression levels of Notch-target genes of freshly isolated (3/4PAR-0h) and cultured (3/4PAR-48h) tissues were examined by qRT-PCR (B). In parallel, the expression of *Hey1* (C and D) and *Gata3* (E and F) was observed in the endoderm of the 3/4PP at qE3 (C and E, respectively) and qE4 (D and F, respectively) by WM-ISH. Schematic drawings in the top/right panels depict the gene-expression domains in the 3PP, the well-defined pouch. *In vitro* (G and H) and *in vivo* (I-L) expression of Notch-target genes in the 3/4PAR with Notch signalling inhibition. Isolated 3/4PAR at qE3 was grown *in vitro* for 48h with three doses of Ly, 50nM (Ly-50), 100nM (Ly-100) and 200nM (Ly-200) (G) or three doses of DBZ, 5μM (DBZ-5), 10μM (DBZ-10) and 15μM (DBZ-15) (H). The expression levels of Notch-target genes were measured in the cultured tissues by qRT-PCR (each transcript in control=1). For the purpose of

Notch signalling inhibition *in vivo*, the right side of cE2.5 embryos were injected in the pharyngeal region with either DMSO (I and K) or Ly (J and L) and allowed to develop *in ovo* for 20-24h. The expression of Notch-target genes, *Hey1* (I and J) and *Gata3* (K and L) was detected by WM-ISH. For qRT-PCR, expression of each transcript was measured as a ratio against the mean of the *Actb* and *Hprt* transcript expression levels and expressed in arbitrary units. Black arrowheads point to the strong hybridisation signals in the 3PP endoderm and white arrowheads point to the pharyngeal arches. A, anterior; cE, chicken embryonic day; D, dorsal; DBZ, Dibenzazepine; Ly, LY-411.575; NG, nodose ganglion; P, posterior; PP, pharyngeal pouch; qE, quail embryonic day; V, ventral. Scale bars, 50μm.

Figure 3. The effects of Notch signalling modulation during T/PT common primordium formation. Timeline of *in vitro* and *in vivo* assays in chicken and quail development (A). *In vitro* (B) and *in vivo* (C-F) expression of thymic, parathyroid and PP endodermal markers in the 3/4PAR. The 3/4PAR at qE3 was mechanically isolated and grown *in vitro* for 48h. Gene-expression levels of freshly isolated (3/4PAR-0h) and cultured (3/4PAR-48h) tissues were examined by qRT-PCR (B). In parallel, *Pax1* (C and D) and *Fgf8* (E and F) expression was detected by WM-ISH in the developing endoderm of the 3/4PP at qE3 (C and E) and qE4 (D and F). Schematic drawings in the top/right panels depict the gene-expression domains in the 3PP, the well-defined pouch. *In vitro* (G and H) and *in vivo* (I-L) expression of thymic, parathyroid and PP endodermal markers in the 3/4PAR with Notch signalling inhibition. Isolated 3/4PAR at qE3 was grown *in vitro* for 48h with three doses of Ly, 50nM (Ly-50), 100nM (Ly-100) and 200nM (Ly-200) (G) or three doses of DBZ, 5μM (DBZ-5), 10μM (DBZ-10) and 15μM (DBZ-15) (H). For Notch signalling *in vivo* assay, the expression of *Foxn1* (I and J) and *Gcm2* (K and L) was observed by WM-ISH in the 3/4PAR of cE3.5 embryos developed for 20-24h after Ly (J and L) or DMSO (I and K) injection. For qRT-PCR, expression of each transcript was measured as a ratio against the mean of *Actb* and *Hprt* transcript expression levels and expressed in arbitrary units. The faint red line delimits the 3PP endoderm. Black arrowheads point to the strong hybridisation signals and white arrowheads point to pharyngeal arches (C and E) or to weak/absent hybridisation signals in the 3/4PP endoderm (J and L). A, anterior; cE, chicken embryonic day; D, dorsal; DBZ, Dibenzazepine; Ly, LY-411.575; P, posterior; PAR, pharyngeal arch region; PP, pharyngeal pouch; qE, quail embryonic day; V, ventral. Scale bars, 50μm.

Figure 4. The effect of early-Notch signalling inhibition in the subsequent formation of the thymus and parathyroid glands. Schematic representation of the 3/4PAR grown *in vitro* for

48h in the absence (3/4PAR Control-200) or presence of 200nM of Ly (3/4PAR Ly-200) and then grafted in the CAM of a cE8 embryo. Explants were allowed to develop *in ovo* for 10 days: Graft-Control, explants grown *in vitro* with DMSO; Graft-Ly, explants grown *in vitro* with Ly (A). The size of thymic lobes (B) and parathyroid glands (I) formed in CAM-derived explants. Serial sections of Graft-Control (C and E; J and L) and Graft-Ly (D and F; K and M) slides were H&E stained (C, D, J and K) and immunodetected with anti-Pan CK antibody and counterstained with Gill's hematoxylin (E, F, L and M). The expression of *Hes5.1* (G and H) and *Foxn1* (G´ and H´) was detected by ISH in serial sections of 3d Graft-Control (G and G´) and Graft-Ly (H and H´) slides. Black arrowheads point to immunoreactive positive cells (E, F, L and M) and to strong hybridisation signals in the endoderm (G-H´). CAM, chorioallantoic membrane; Expl, explants; PAR, pharyngeal arch region; PT, parathyroid glands; TL, thymic lobe; 10d, ten days; 3d, three days. Scale bars, 50μm.

Figure 5. Crosstalk of Notch and Hh signalling pathways during T/PT common primordium formation. *In vitro* (A) and *in vivo* (B-G) expression of Hh-related genes in the 3/4PAR. The 3/4PAR at qE3 was mechanically isolated and grown *in vitro* for 48h. Gene-expression levels of freshly isolated (3/4PAR-0h) and cultured (3/4PAR-48h) tissues were examined by qRT-PCR (A). In parallel, *Patched1* (B and E), *Gli1* (C and F) and *Gli3* (D and G) expression was observed in the developing endoderm of the 3/4PP at qE3 (B-D) and qE4 (E-G). Schematic drawings in the top/right panels depict the gene-expression domains in the 3PP, the well-defined pouch. Notch (H and I) and Hh (J and K) inhibition *in vitro* assays. Expression levels of Hh-related (H, I and K) and Notch-related (J) genes in 3/4PAR grown *in vitro* for 48h in the presence of Ly (H), DBZ (I), Cyc and Vis (J and K) were examined by qRT-PCR. Expression of each transcript was measured as a ratio against the mean of the *Actb* and *Hprt* transcript expression levels and expressed in arbitrary units (each transcript in control=1). Black arrowheads point to the hybridisation signals in the 3/4PP endoderm (D and G). A, anterior; Cyc, Cyclopamine; D, dorsal; DBZ, Dibenzazepine; Ly, LY-411.575; P, posterior; PAR, pharyngeal arch region; PP, pharyngeal pouch; qE, quail embryonic day; V, ventral; Vis, Vismodegib. Scale bars, 50μm.

Figure 6. The effect of *in vivo* Hh signalling inhibition during T/PT common primordium formation. PBS-beads (A-D and M) and Cyc-beads (E-H and N) were implanted in the pharyngeal region of cE2.5 (A, B, D-F and H) and qE3 (C, G, M and N) and embryos allowed to develop for 20-24h. Expression of *Gata3* (A, C, E and G), *Gcm2* (B and F), *Lfng* (D and H) and *Foxn1* (M and N) was observed by WM-ISH. In parallel, the expression of *Notch1* (I),

Delta1 (K) and *Jag1* (L) was examined in the pharyngeal region of cE3. Timeline of *in vivo* assays in chicken and quail development (J). Faint red line delimits the 3PP endoderm. Black and white arrowheads point to strong and weak/absent hybridisation signals in the PP endoderm, respectively. A, anterior; cE, chicken embryonic day; Cyc, cyclopamine; D, dorsal; P, posterior; PP, pharyngeal pouch; qE, quail embryonic day; V, ventral. Scale bars, 50μm.

Figure 7. Model of Hh and Notch signalling modulation during thymic and parathyroid rudiment formation. Schematic representation of the results obtained during *in vivo* and *in vitro* assays (A). Cross sections of the most ventral region of the embryo and expression of T/PT markers, Notch-target genes and Shh in 3PP endoderm during normal development and when Notch and Hh signalling is inhibited (A). Expression of *Shh* in isolated pharyngeal endoderm examined by WM-ISH at cE3.5 and cE4.5 (B). Schematic model of Notch and Hh signalling crosstalk during T/PT common primordium formation during normal development and in the absence of Hh signalling (C). In detail is depicted a proposed model for the lateral inhibition mechanism involved in the median/posterior thymic boundary definition. In this case, the relative levels of Notch and Delta determine the cell's signalling state. The cell with more Notch than Delta becomes a 'receiver' and cells with more Delta than Notch become 'sender' cells. In the absence of Hh, reduction of the Delta1 signalling gradient shifts the boundary to a more median position within the pouch. Arrows indicate putative signalling crosstalk (see Discussion for details). A, anterior; cE, chicken embryonic day; D, dorsal; D>N, Delta>Notch; N>D, Notch>Delta; P, posterior; PP, pharyngeal pouch; qE, quail embryonic day; V, ventral. Scale bars, 100μm.

Table 1. List of primers used in qRT-PCR assays.

Primer	Forward primer (5'-3')	Reverse primer (5'-3')	Product size (bp)
ACTB	TGGCACCTAGCACAATGAAA	GCCAGGATAGAGCCTCCAAT	82
HPRT	ACGCCCTCGACTACAATGAA	CAACTGTGCTTTCATGCTTTG	98
Foxn1	CGACATCGATGCTCTGAATC	AGGCTGTCATCCTTCAGCTC	81
Gcm2	TCAGAATTCCCAGAAAAAGAGA	GAGGGCAGATTTTGCATGTT	93
PTH	CTGATGGAAGACCAATGATGAA	AAGCCAGTCCTGTCTCTCCA	98
Gata3	CTGTAATGCCTGTGGGCTCT	CATTTTTCGGTTTCTGGTCTG	94
Pax1	GGGAAGTCACGGACAGAAAA	GGATCGAGAGTCCGTGGAT	81
Fgf8	GCATGAACAAGAAGGGGAAA	AGCGCCGTGTAGTTGTTCTC	97
Hey1	ACCGTGGATCACCTGAAGAT	CGGTAGTCCATAGCCAAAGC	80
Hes5.1	CCGACATCCTGGAGATGACT	AGGCATACCCTTCGCAGTAA	99
Hes6.1	GGAGGTGCTGGAGCTGAC	GCATGCACTGGATGTAGCC	122
Patched1	GGAAGCCACTGAGAATCCTG	TGCAATCTGGGACTTGACTG	81
Shh	CGGCTTCGACTGGGTCTACT	ATTTCGCTGCCACTGAGTTT	80
Gli1	AAGGATGACGGCAAGCTG	GTCACTGCTGCACGATGACT	86
Gli3	TGGAATGCTTCCAAGACTGA	CTGCAGCTGCTGTTTGATTG	96

Highlights

- Notch is required for thymic epithelium specification.
- Notch positively regulates parathyroid epithelium differentiation.
- Hh positively regulates Gata3/Gcm2/parathyroid-fate domain.
- Hh positively regulates Lfng-domain in the 3/4PP.
- Hh establishes the dorsal/posterior boundary of Foxn1/thymic rudiment.

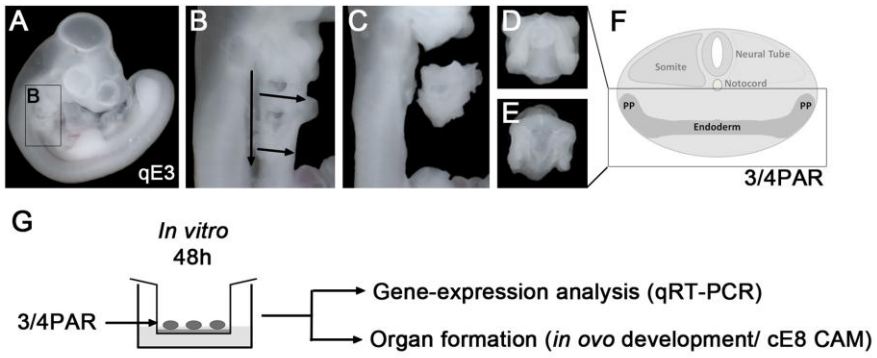

Figure1_Figueiredo et al.

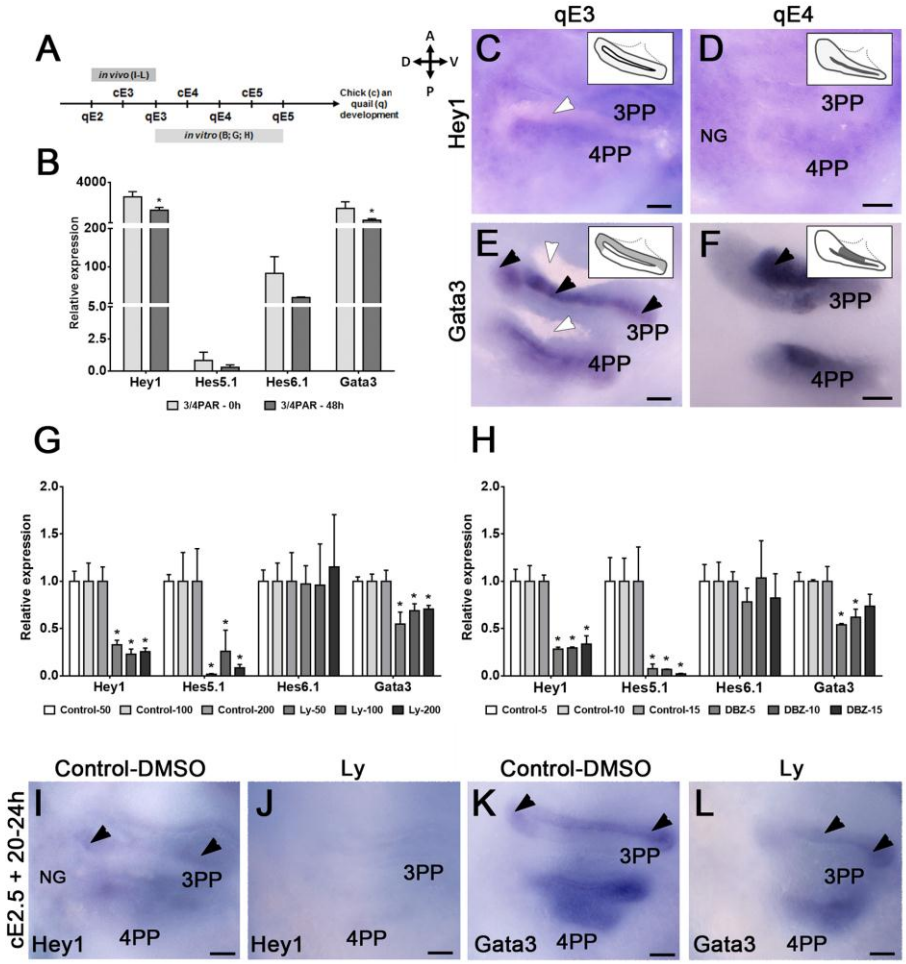

Figure 2_Figueiredo et al.

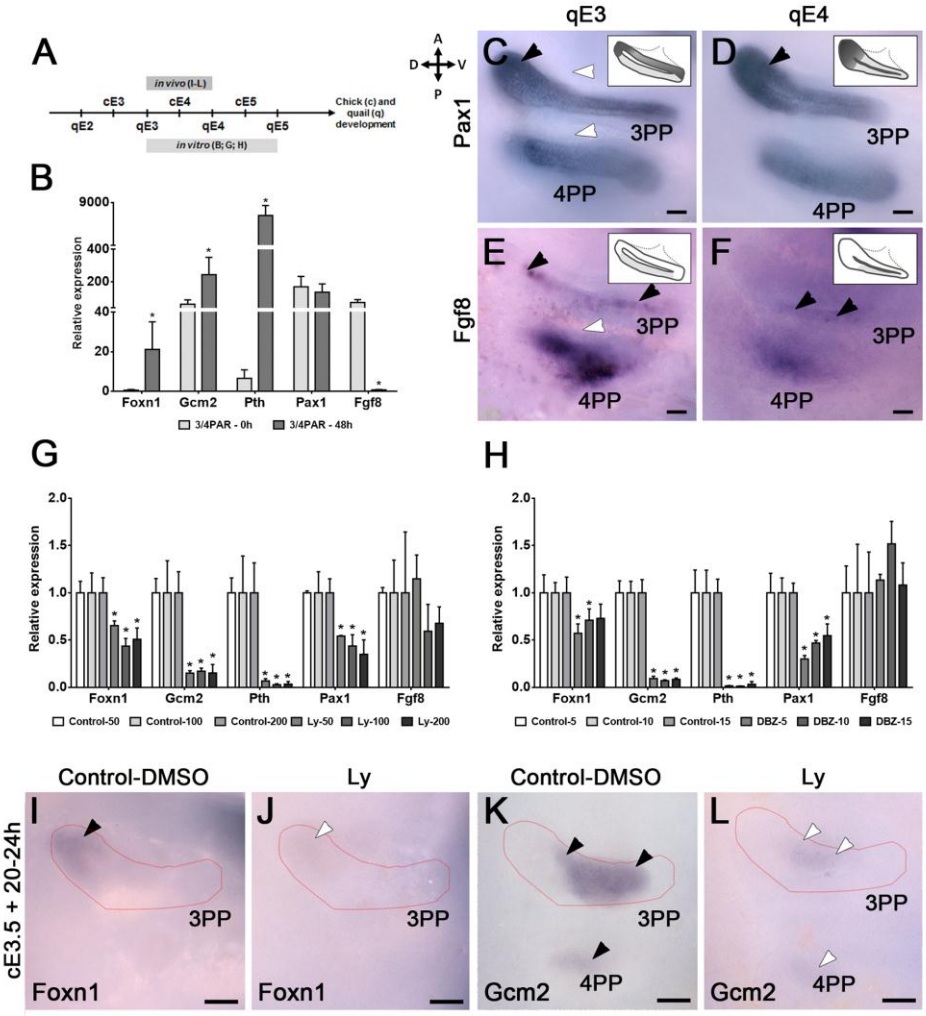

Figure 3_Figueiredo et al.

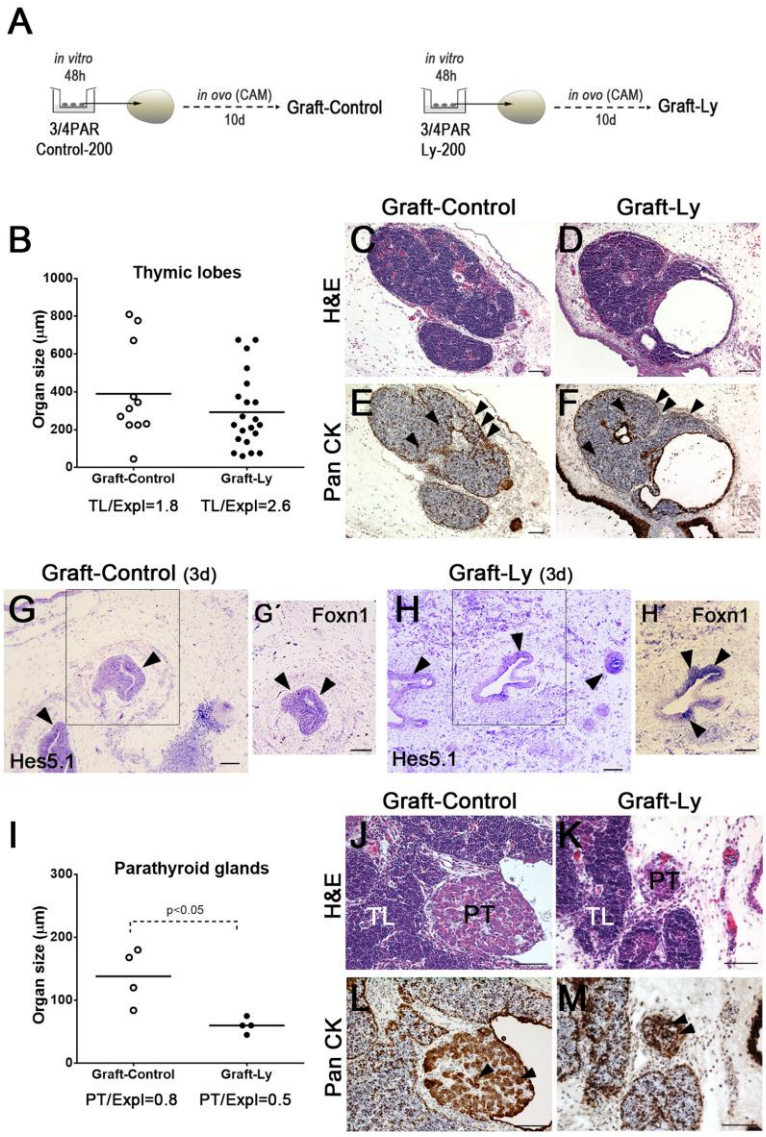

Figure 4_Figueiredo et al.

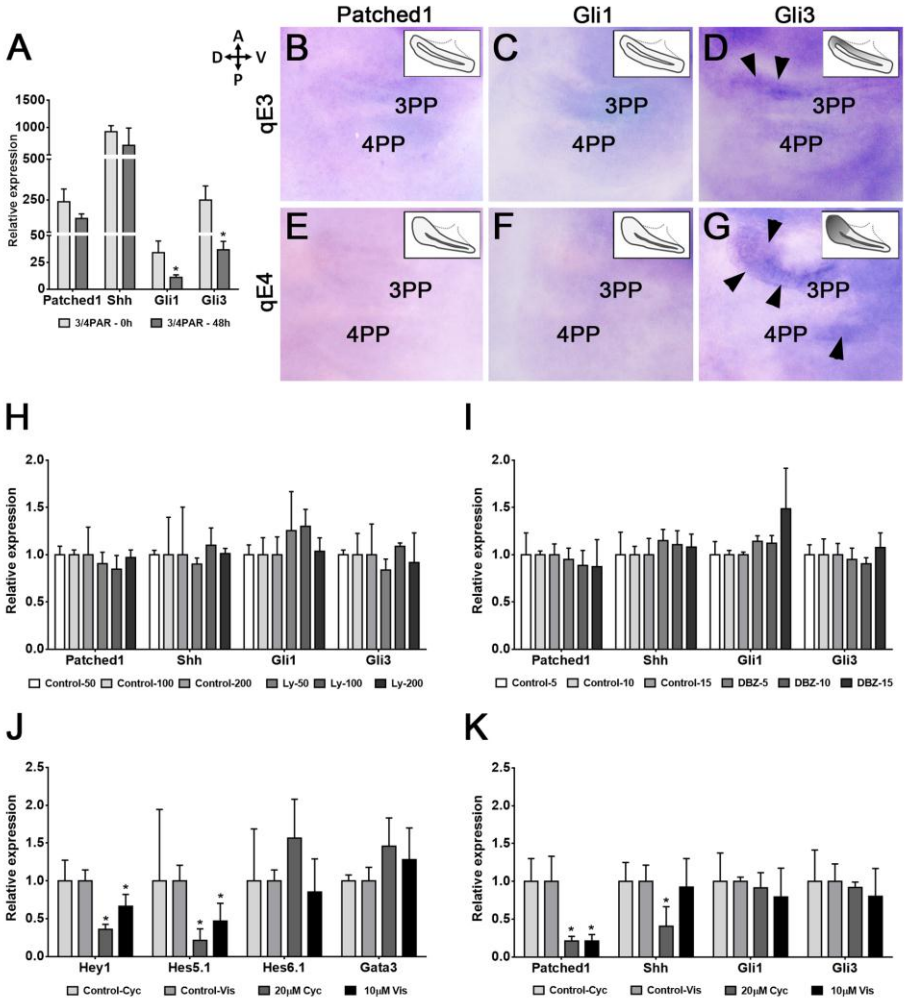

Figure 5_Figueiredo et al.

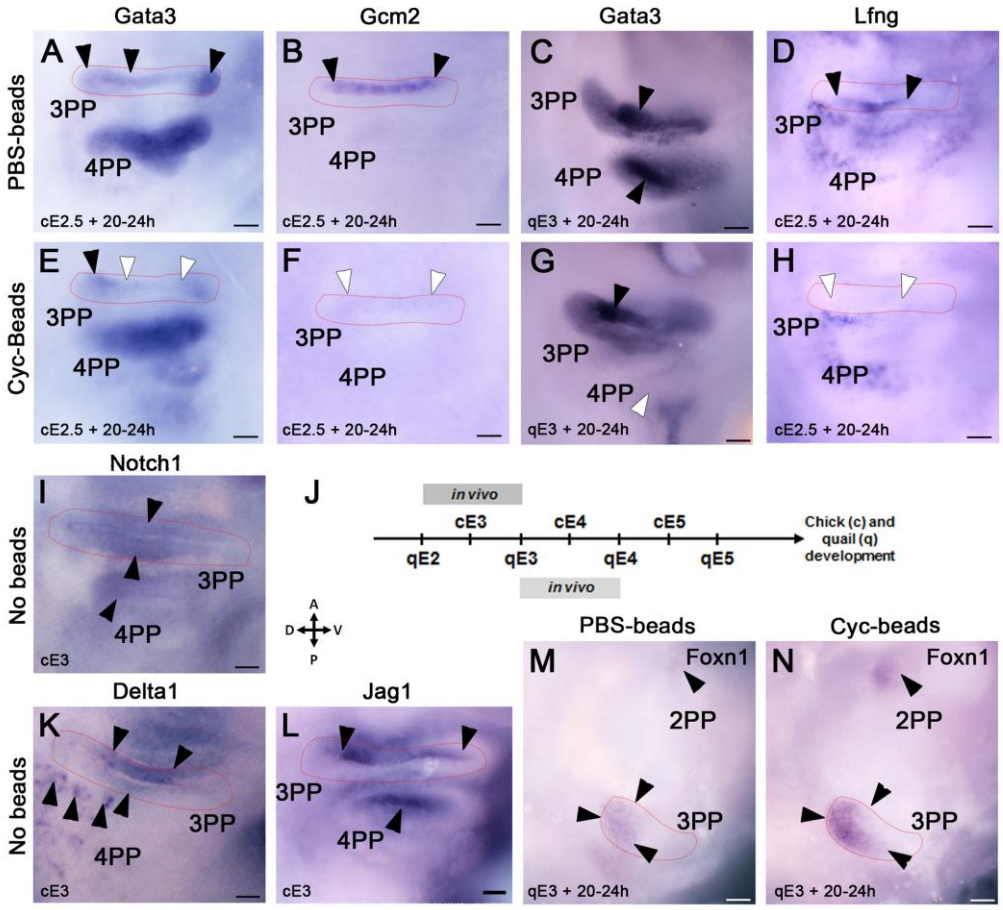

Figure 6_Figueiredo et al.

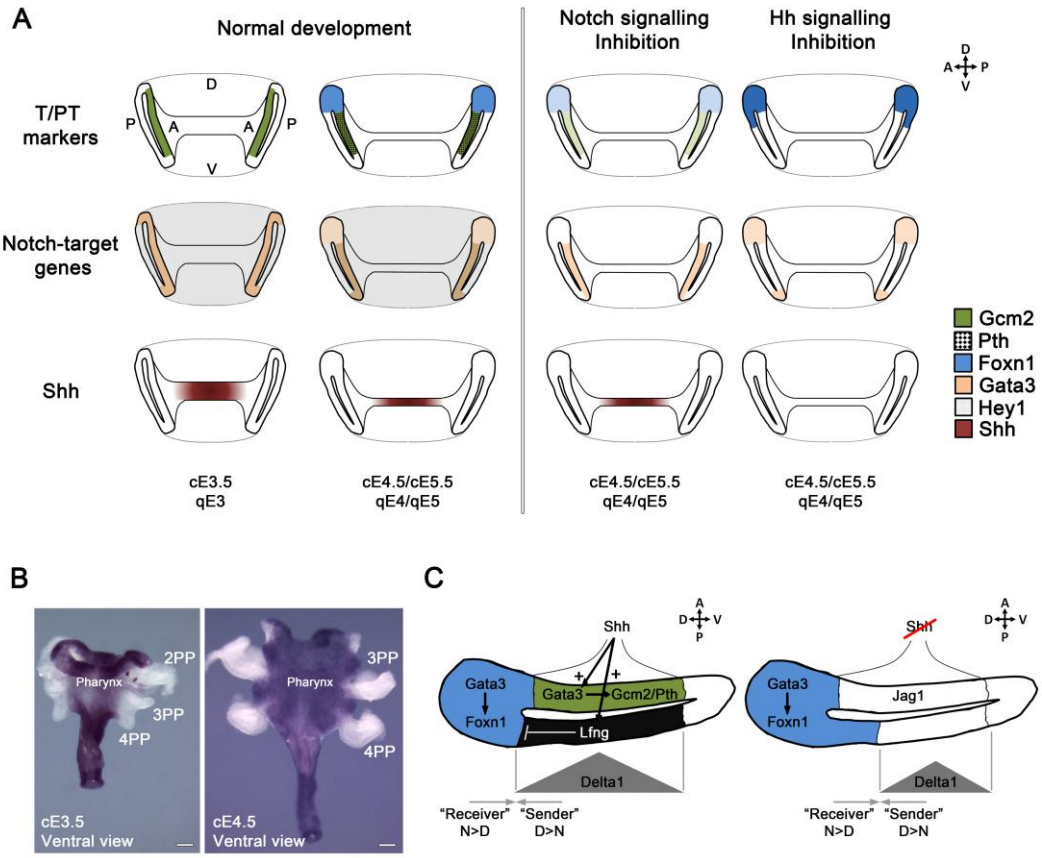

Figure 7_Figueiredo et al.